

Application of Split TCSC for Fine Power Flow Control

P. Surajith Reddy¹, K. Anil Kumar Reddy²

¹M.Tech student, Electrical Department, JNTUA College of Engineering, Anantapur, India.

²M.Tech student, Electrical Department, JNTUA College of Engineering, Anantapur, India.

Abstract: A Thyristor controlled series capacitor (TCSC) device is one among the flexible AC transmission system (FACTS) devices which is capable of controlling the line impedance with introduction of a thyristor controlled reactor (TCR) in parallel with fixed capacitor. The TCSC device provides inductive and capacitive reactance compensation to make changes in the power flow of the transmission line. In tuning the TCSC, a difficulty is observed i.e., for small change in firing angle there is large change in reactance offered by TCSC near resonance region which makes inconvenience at load end for compensating small change in dynamic demand.

This paper presents fine-tuning of line reactance by using split TCSC over single TCSC. The Newton-Raphson method of power flow analysis (NRPFA) is used to analyze the fine-tuning of line reactance for compensation of small change in the power demand. Comparison of percentage change in reactance offered at various firing angles. Comparison of real power flow and power loss variations among split TCSC and single TCSC are carried out on standard IEEE 30-bus system and IEEE 14-bus system. In addition, Available Transfer Capacity (ATC) is also observed for the power system using the Continuation Power Flow (CPF) for base case and after the placement of the TCSC. The IEEE 14 bus system and IEEE 30 bus system are taken as a case study power systems.

Keywords: Split TCSC, Single TCSC, Newton Raphson power flow analysis, Available Transfer Capability.

1. INTRODUCTION

In developing countries, there is unpredictable increase in power demand commercially and industrially; there by providing quality and procure power to the consumers become a difficult task. Due to this increase in power demand, power transmission system has to maintain reliability and security during transmission of power. The rise in demand can be met by construction of additional transmission lines to provide more power. But construction of new transmission lines in addition is not a economical thing due to cost included in erecting towers, insulators and conductors. Using fixed capacitors which provide fixed series compensation is a economic technique compared to construction of additional transmission lines which was first used in USA. With the advent of power electronics smooth variation of compensation came in to existence instead of fixed series compensation.

Among Flexible AC Transmission system (FACTS) devices, the Thyristor Controlled Series Capacitor (TCSC) device reduces the transmission line reactance. The reduced value of transmission line reactance enhances the active power flow in the transmission line and may be loaded up to thermal limits without incurring more loss in the line. These features of TCSC device enhance the transmission system to transfer the desired power at right line [3-7]. Many TCSC projects are installed worldwide and are operational [8]. The Slatt TCSC project is unique in the sense that has Six TCSC modules connected in series. Application of multiple TCSC [9,10] has given the idea of splitting the degree of compensation(k) which has benefits of power flow improvement and thus application of split TCSC is used in the transmission line over single TCSC. Mohan Mathur and Varma [4] presented that the reactance vs current (X-I) capability curves for multi modules of TCSC reveals feasible combination of tuning multi TCSC providing microtuning of net reactance in the line. from the single TCSC reactance characteristic curve It is observed that small change in reactance ΔX with increase in firing angle (α) of TCSC thyristors but near resonance region each step of a firing angle makes a huge elapse of reactance. Hence proper tuning of reactance is not possible.

The paper organized as follows: The operation of single TCSC and split TCSC device are schematically and mathematically explained in Sections 2 and 3. The mathematical modeling of Newton Raphson method Power flow analysis (NRPFA) with single TCSC and split TCSC are discussed in Section 4. Section 5 optimally chooses the place for TCSC with loss sensitivity index analysis. Calculation of ATC for TCSC is discussed in section 6. Results and analysis is discussed in section 7. Conclusion is discussed in section 8

2. OPERATION OF SINGLE TCSC AND SPLIT TCSC

2.1. Single TCSC

The schematic diagram of TCSC device is shown in Fig 1. by which basic operation of TCSC device can be explained. TCSC device consists of series capacitor and thyristor controlled reactor connected in parallel and TCR is controlled by firing angle α [3,4].

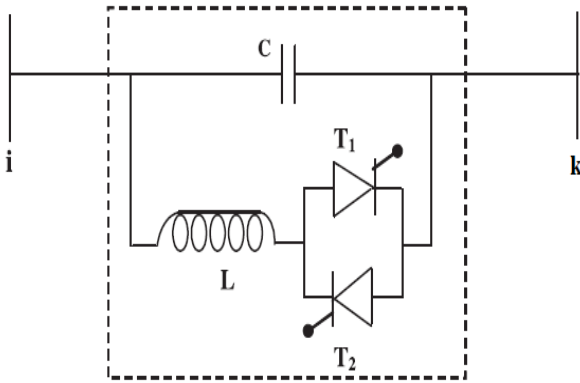


Fig-1: Thyristor Controlled Series Capacitor (TCSC)

Fig. 2 shows the reactance characteristics curve of a TCSC device drawn between effective reactance of TCSC and firing angle α . The effective reactance ' $X_{TCSC}(\alpha)$ ' of TCSC operates in three region: inductive region, capacitive region and resonance region. Inductive region starts increasing from inductive reactance $X_L || X_c$ value to infinity (parallel resonance condition, ' $X_L(\alpha)=X_c$ '), and decreasing from infinity to capacitive reactance X_C for capacitive region. Between the two regions, resonance occurs [3,4].

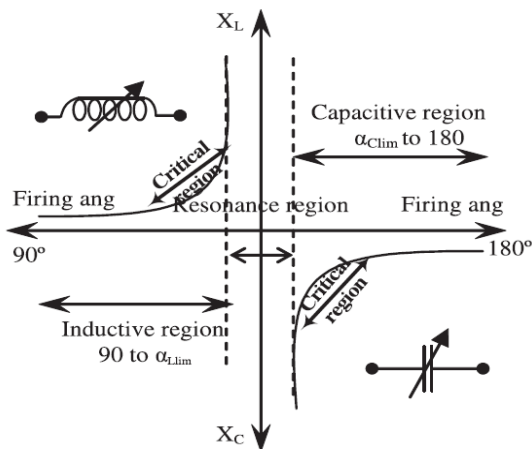


Fig-2: Reactance characteristics curve of a TCSC

The reactance characteristics of TCSC shows, operation in both capacitive and inductive regions through variation of firing angle (α) as shown below:

Range of firing angle	Region
$90 \leq \alpha \leq \alpha_{Lim}$	Inductive region
$\alpha_{clim} \leq \alpha \leq 180$	Capacitive region
$\alpha_{Lim} \leq \alpha \leq \alpha_{clim}$	Resonance region

While tuning the TCSC device in critical region a large change in reactance ΔX is observed in the reactance characteristic curve as shown in Fig. 2. Due to large change in reactance, flexibility in power flow becomes rigid. Therefore, it is inconvenient to tune between those reactances and difficult to compensate for any fine change in dynamic demands on load side.

2.2. Split TCSC

To avoid above difficulty and to utilize the full range of reactance, use of split TCSC device for the same amount of compensation (k) is proposed. Fig. 3 shows a split TCSC in place of single TCSC for same compensation. The degree of compensation k of single TCSC can be splitted in to two: k_1 and k_2 and values are chosen depending on the requirement of power compensation power oscillations in the line. The deployment of more than two TCSC in the line adds to complexity in control. By implementing fine-tuning on both the TCSC's, the split TCSC can maintain precise control on power flow over the line and even the small increment/decrement of demand can be conveniently met. The TCSC has four normal modes of operation such as blocking mode, bypass mode, vernier inductive mode and vernier capacitive mode [4]. Additionally one more mode is possible which is known as cutoff mode. By making any one TCSC in cutoff mode, other can be tuned [12].

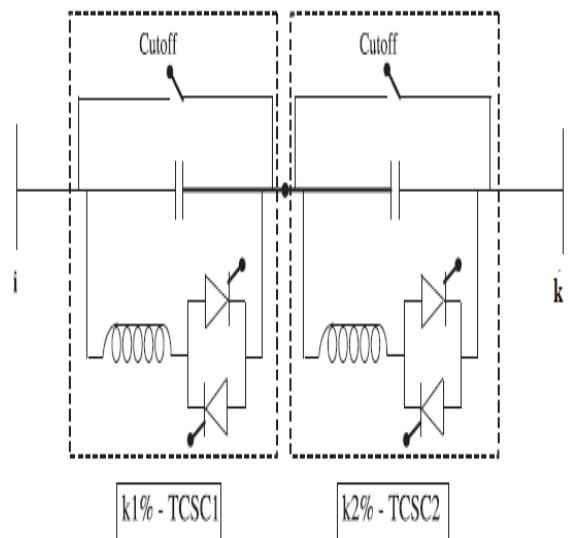


Fig-3: Split TCSC in a transmission line

3. MATHEMATICAL MODELING OF TCSC

3.1. Modeling of single TCSC

A TCSC is a series type FACTS device; inserted for line reactance compensation in the transmission line between 'i' and 'k' as shown in Fig. 4.

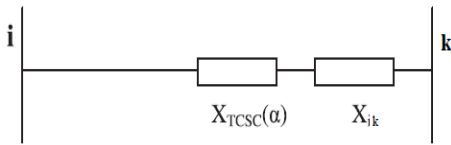


Fig-4: Transmission line with split TCSC

TCSC can operate either in inductive mode or in capacitive mode. (+) Sign is for inductive reactance and (-) sign for capacitive reactance. So the net reactance of the transmission line becomes [4,13]

$$X_{Total} = X_{ik} \pm X_{TCSC}(\alpha) \quad (1)$$

Where α is the firing angle of TCSC varies from 90° to 180° .

Effective TCSC reactance X_{TCSC} with respect to firing angle (α) can be given as:

$$X_{TCSC}(\alpha) = -X_c + C_1(2(\pi - \alpha) + \sin(2(\pi - \alpha))) - C_2 \cos^2(\pi - \alpha) (\omega \tan(\omega(\pi - \alpha)) - \tan(\pi - \alpha)) \quad (2)$$

where

$$C_1 = \frac{X_c + X_L}{\pi}$$

$$C_2 = 4 \frac{1}{X_L \pi} \left(\frac{X_c X_L}{X_c - X_L} \right)^2$$

$$\omega = \sqrt{\frac{X_c}{X_L}}$$

3.2. Modeling of split TCSC

Fig. 5 shows the split TCSC is connected in the transmission line between the buses i and k. The split TCSC is a combination of

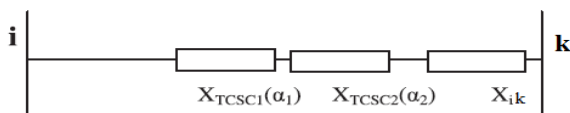


Fig-5: Transmission line with split TCSC

two single TCSC; but splitted in terms of ratio of degree of series compensation ($k = k_1 + k_2$). The degree of series compensations k_1 and k_2 are appropriately chosen to get wide and fine reactance compensation in the network. Both the TCSC's are efficiently tuned and fine tuning of line reactance are achieved. Thus, the net line reactance becomes,

$$X_{Total} = X_{ik} \pm X_{TCSC1}(\alpha_1) \pm X_{TCSC2}(\alpha_2) \quad (3)$$

where α_1 and α_2 are firing angles of split TCSC, each can be tuned separately between 90° to 180° .

Considering 'n' number of possible firing steps between 90° to 180° , $[n \times n]$ firing points are possible for split TCSC.

Apart from tuning, each TCSC can operate alone in cutoff mode. So that $[(n + 1) \times (n + 1)]$ reactances are possible for compensation.

$$X_{Total} = X_{ik} \pm X_{se} [(\alpha_{1,n+1})x(\alpha_{2,n+1})] \quad (4)$$

$$X_{se} [\alpha_{1(n+1)}, \alpha_{2(n+1)}] = \begin{bmatrix} X_{se}(1,1) & \dots & X_{se}(1,1) & X_{TCSC2}(1) \\ \vdots & \ddots & \vdots & \vdots \\ X_{se}(1,1) & \dots & X_{se}(1,1) & X_{TCSC2}(n) \\ X_{TCSC1}(1) & \dots & X_{TCSC1}(n) & \text{Both in cutoff} \end{bmatrix} \quad (5)$$

where $X_{se}(N_1, N_2) = [X_{TCSC1}(N_1) \pm X_{TCSC1}(N_2)]$, both N_1 and N_2 varies from 1 to n.

Hence, fine tuning of reactance is possible by splitting the TCSC device.

4. MATHEMATICAL MODELING OF NRPFA METHOD

4.1. Modeling of NRPFA with single TCSC:

Newton Raphson method power flow analysis (NRPFA) is used to analyze regarding the fine control of line reactance in transmission line. The analysis is implemented for lumped π equivalent model of transmission line with single TCSC device as shown in Fig.6.

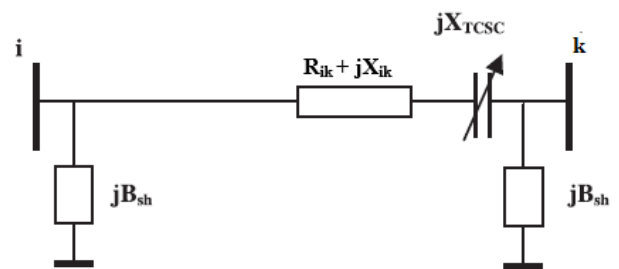


Fig-6: Equivalent model of transmission line with single TCSC

The transmission line has its own equivalent resistance, reactance and shunt susceptance of R_{ik} , X_{ik} and B_{sh} . A static model of TCSC device is connected between the buses i and k. So the line reactance X_{ik} can be varied by capacitive or inductive mode operation of TCSC. The TCSC's capacitive mode of operation decreases the line reactance whereas inductive mode of operation increases line reactance. Thus the variation in reactance manages the real and reactive power flows in the transmission line [16]. Between the buses i and k change in the line admittance ($\Delta Y'_{ik}$) is

$$\Delta Y'_{ik} = Y'_{ik} - Y_{ik} = (G'_{ik} + jB'_{ik}) - (G_{ik} + jB_{ik}) \quad (6)$$

where

$$G_{ik} = \frac{R_{ik}}{R_{ik}^2 + X_{ik}^2}$$

$$G'_{ik} = \frac{R_{ik}}{R_{ik}^2 + (X_{ik} + X_{TCSC})^2}$$

$$B_{ik} = \frac{-X_{ik}}{R_{ik}^2 + X_{ik}^2};$$

$$B'_{ik} = -\frac{X_{ik} + X_{TCSC}}{R_{ik}^2 + (X_{ik} + X_{TCSC})^2}$$

After placement of TCSC device in the transmission line, net admittance or Y_{bus} ' becomes,

$$Y'_{bus} = Y_{bus} + \Delta Y'_{bus} = Y_{bus} + \begin{bmatrix} 0 & 0 & 0 & 0 & 0 & 0 \\ 0 & \Delta Y'_{ik} & 0 & 0 & -\Delta Y'_{ik} & 0 \\ 0 & 0 & 0 & 0 & 0 & 0 \\ 0 & 0 & 0 & 0 & 0 & 0 \\ 0 & -\Delta Y'_{ik} & 0 & 0 & \Delta Y'_{ik} & 0 \\ 0 & 0 & 0 & 0 & 0 & 0 \end{bmatrix}$$

Hence the updated Y'_{ik} can be directly used in Newton Raphson method power flow analysis for calculation of power distributions in the network. For every location of TCSC device between the buses i and k , the change in admittance ($\Delta Y'_{ik}$) is placed at corresponding self and mutual admittance shells of $\Delta Y'_{bus}$ matrix as in [12].

Power flow in the transmission lines with TCSC are,

$$S_{ik} = P_{ik} - jQ_{ik} = V_i * I_{ik} = V_i^2 [G'_{ik} + j(B'_{ik} + B_{sh})] - V_i * V_k (G'_{ik} B'_{ik}) \quad (7)$$

The real and reactive power flows between the buses i and k are

$$\begin{aligned} P_{ik} &= V_i^2 G'_{ik} - V_i V_k G'_{ik} \cos(\delta_i - \delta_k) - V_i V_k B'_{ik} \sin(\delta_i - \delta_k) \\ P_{ki} &= V_k^2 G'_{ik} - V_i V_k G'_{ik} \cos(\delta_i - \delta_k) + V_i V_k B'_{ik} \sin(\delta_i - \delta_k) \end{aligned} \quad (8)$$

and

$$Q_{ik} = -V_i^2 (B'_{ik} + B_{sh}) - V_i V_k G'_{ik} \sin(\delta_i - \delta_k) + V_i V_k B'_{ik} \cos(\delta_i - \delta_k) \quad (9)$$

$$Q_{ki} = -V_k^2 (B'_{ik} + B_{sh}) + V_i V_k G'_{ik} \sin(\delta_i - \delta_k) + V_i V_k B'_{ik} \cos(\delta_i - \delta_k) \quad (10)$$

Therefore power losses are,

$$\begin{aligned} S_L &= S_{ik} + S_{ki} = P_L + jQ_L \\ P_L &= P_{ik} + P_{ki} = [V_i^2 + V_k^2 - 2V_i V_k \sin(\delta_i - \delta_k)] G'_{ik} \end{aligned} \quad (11)$$

$$Q_L = Q_{ik} + Q_{ki} = -V_i^2 (B'_{ik} + B_{sh}) - V_k^2 (B'_{ik} + B_{sh}) + 2V_i V_k B'_{ik} \cos(\delta_i - \delta_k) \quad (12)$$

Real and reactive powers injected by TCSC are

$$P_{TCSC} = V_i^2 \Delta G_{ik} - V_i V_k \Delta G_{ik} \cos(\delta_i - \delta_k) - V_i V_k \Delta B_{ik} \sin(\delta_i - \delta_k)$$

$$P_{TCSC} = V_k^2 \Delta G_{ik} - V_i V_k \Delta G_{ik} \cos(\delta_i - \delta_k) + V_i V_k \Delta B_{ik} \sin(\delta_i - \delta_k) \quad (13)$$

and

$$\begin{aligned} Q_{TCSC} &= -V_i^2 \Delta B_{ik} - V_i V_k \Delta G_{ik} \sin(\delta_i - \delta_k) + V_i V_k \Delta B_{ik} \cos(\delta_i - \delta_k) \\ Q_{TCSC} &= -V_k^2 \Delta B_{ik} + V_i V_k \Delta G_{ik} \sin(\delta_i - \delta_k) + V_i V_k \Delta B_{ik} \cos(\delta_i - \delta_k) \end{aligned} \quad (14)$$

4.2. Modeling of NRPFA with split TCSC:

Fig.7 shows the transmission line with split TCSC in lumped π equivalent model. With split TCSC between the buses i and k change in the line admittance ($\Delta Y'_{ik}$) is

$$\Delta Y'_{ik} = Y'_{ik} - Y_{ik} = (G'_{ik} + jB'_{ik}) - (G_{ik} + jB_{ik}) \quad (15)$$

where

$$\begin{aligned} G_{ik} &= \frac{R_{ik}}{R_{ik}^2 + X_{ik}^2}; \\ G'_{ik} &= \frac{R_{ik}}{R_{ik}^2 + (X_{ik} + X_{TCSC}(\alpha_1) + X_{TCSC}(\alpha_2))^2} \\ B_{ik} &= \frac{-X_{ik}}{R_{ik}^2 + X_{ik}^2}; \\ B'_{ik} &= -\frac{X_{ik} + X_{TCSC}(\alpha_1) + X_{TCSC}(\alpha_2)}{R_{ik}^2 + (X_{ik} + X_{TCSC}(\alpha_1) + X_{TCSC}(\alpha_2))^2} \end{aligned}$$

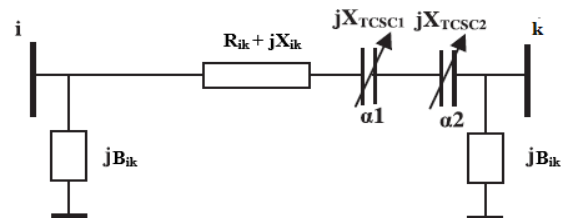


Fig-7: Equivalent model of transmission line with split TCSC

After placing split TCSC in the transmission line, net admittance or Y'_{bus} becomes

$$Y'_{bus} = Y_{bus} + \Delta Y'_{bus} = Y_{bus} + \begin{bmatrix} 0 & 0 & 0 & 0 & 0 & 0 \\ 0 & \Delta Y'_{ik} & 0 & 0 & -\Delta Y'_{ik} & 0 \\ 0 & 0 & 0 & 0 & 0 & 0 \\ 0 & 0 & 0 & 0 & 0 & 0 \\ 0 & -\Delta Y'_{ik} & 0 & 0 & \Delta Y'_{ik} & 0 \\ 0 & 0 & 0 & 0 & 0 & 0 \end{bmatrix}$$

5. LOSS SENSITIVITY ANALYSIS

The TCSC devices are optimally injected in the transmission line for distributing the powers in the network [17-21]. Abdel-Moamen [17] presented a paper on optimal power flow incorporates single/multi TCSC devices using spare Newton's algorithms.

Its main aim is to minimize transmission line losses. Mahdad et al. [18] and Biansoongnern et al. [19] applied system load ability and loss minimization method to optimally select the placement of TCSC. The reactive powers are optimally dispatched by using FACTS devices which are selected based on loss sensitivity method.

The sensitivity method uses line reactance X_{ik} of the transmission line as a control variable for placing the TCSC device. Thus, the real and reactive power loss of sensitivity method with respect to the control variable X_{ik} can be given as,

$$a_{ik} = \frac{\partial P_L}{\partial X_{ik}} = \text{Real power loss sensitivity index}$$

and

$$b_{ik} = \frac{\partial Q_L}{\partial X_{ik}} = \text{Reactive power loss sensitivity index}$$

The real and reactive power loss on each line can be formulated as

$$P_L = P_{ik} + P_{ki} = [V_i^2 + V_k^2 - 2V_i V_k \sin(\delta_i - \delta_k)] G'_{ik} \quad (16)$$

$$Q_L = Q_{ik} + Q_{ki} = -V_i^2 (B'_{ik} + B_{sh}) - V_k^2 (B'_{ik} + B_{sh}) + 2V_i V_k B'_{ik} \cos(\delta_i - \delta_k) \quad (17)$$

The loss sensitivity indices a_{ik} and b_{ik} can be derived from eqn. (16) and eqn. (17) as

$$a_{ik} = \frac{\partial P_L}{\partial X_{ik}} = (V_i^2 + V_k^2 - 2V_i V_k \cos(\delta_i - \delta_k)) \frac{2R_{ik} X_{ik}}{(R_{ik}^2 + X_{ik}^2)^2} \quad (18)$$

$$b_{ik} = \frac{\partial Q_L}{\partial X_{ik}} = (V_i^2 + V_k^2 - 2V_i V_k \sin(\delta_i - \delta_k)) \frac{R_{ik}^2 - X_{ik}^2}{(R_{ik}^2 + X_{ik}^2)^2} \quad (19)$$

The criteria for optimal placement of FACTS device are on the most sensitive line. The TCSC should be kept in a line having the most positive loss sensitivity index. Also TCSC should not be injected between two generator buses, even though the line sensitivity is large [16, 17].

Loss sensitivity indices are calculated on standard power systems and among the systems most sensitive line is identified. The optimal location for placing TCSC device is at transmission line which is mentioned on above test systems. The single TCSC and split TCSC device are alternatively placed in this transmission line and power flows in the transmission line are analyzed from 90° to 180° of firing angle.

6. ATC CALCULATION OF TRANSMISSION NETWORK

Available Transfer Capability (ATC) is a measure of the transfer capability remaining in the physical

transmission network for further commercial activity over and above already committed uses. Mathematically, ATC is defined as the Total Transfer Capability (TTC) less the Transmission Reliability Margin (TRM), less the sum of existing transmission

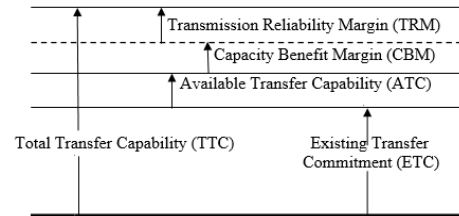


Fig-8: Basic Definition of ATC

commitments (which includes retail customer service) and the Capacity Benefit Margin (CBM), shown in Fig.8 [24]. Total Transfer Capability (TTC) is defined as the amount of electric power that can be transferred over the interconnected transmission network in a reliable manner while meeting all of a specific set of defined pre- and post-contingency system conditions. Mathematically, ATC is defined as [24]:

$$ATC = TTC - \{TRM + \{ETC + CBM\}\}$$

There are so many methods to compute ATC. In ref. [25], the topological information of a system is stored in a matrix form and constants for different simultaneous cases and critical contingencies have been calculated beforehand and used for determination of ATC values. For very large systems, the method may be quite cumbersome. In ref. [25], the localized linearity of the system is assumed and additional loading required to hit the different transfer limits are separately calculated and the minimum of all these is taken as the ATC. The ATC is calculated by the following methods.

1. Method based on Continuation Power Flow.
2. Method based on distribution factors.

6.1 Method based on Continuation Power Flow (CPF)

From the solved base case, power flow solutions are sought for increasing amounts of transfer in the specified direction [26]. The quantity of the transfer is a scalar parameter, which can be varied in the model. The amount of transfer is gradually increased from the base case until a binding limit is encountered. This continuation process requires a series of power system solutions to be solved and tested for limits. The transfer capability is the change in the amount of transfer from the base case transfer at the limiting point. Continuation can be simply done as a series of load flow calculations

for increasing amounts of transfers. However, when convergence could be poor, such as the case for transfers approaching voltage instability, methods that allow the transfer parameter to become a dependent variable of the model are the most successful. Continuation Power Flow (CPF) is a method for finding the maximum value of a scalar parameter in a linear function of changes in injections at a set of buses in a power flow problem [25]. Originally introduced for determining maximum load ability, CPF is adaptable, without change in principle, for other applications, including ATC. The CPF algorithm effectively increases the controlling parameter in discrete steps and solves the resulting power flow problem at each step. The procedure is continued until a given condition or physical limit preventing further increase is reached. Because of solution difficulty and the need for the jacobian matrix at each step, the Newton power flow algorithm is used. CPF yields solution even at voltage collapse points. A continuation power flow is performed by starting from an initial point and then increasing the load by a factor until some system limit is reached. The loads are defined as:

$$P_{Li} = \lambda P_{Loi}$$

$$Q_{Li} = \lambda Q_{Loi}$$

Where

P_{Loi} , Q_{Loi} , are the active and reactive power respectively of bus i in the base case;

P_{Li} , Q_{Li} are the active and reactive power of bus i increased by parameter λ .

For a specific source/sink transfer case calculation of the ATC may be summarized as the maximum transfer power without causing a limit violation over the base case.

7. RESULTS AND ANALYSIS

7.1. Optimal placement of TCSC

Loss sensitivity indices are calculated on IEEE 14 bus system and the most sensitive line among the system is identified using the method discussed in section 5. The optimal location for installing TCSC device is at transmission lines 19 on above mentioned test system.

The single TCSC and split TCSC device are alternatively placed in these transmission lines and power flows in the transmission lines are examined from 90° to 180° of firing angle.

7.2 Design of single TCSC and split TCSC

For the single TCSC design, the degree of compensation ' k ' and ' ω ' are considered as 10% and 2.4% respectively to get single resonance region. The firing angle limitation under resonance region is considered from 137° to 148° where TCSC should not be tuned.

Fig. 7.1 shows the single TCSC reactance characteristics curve plotted in steps of 1° firing angle. Same reactance characteristics curve is plotted against number of firing points (0 – 91) is shown in Fig. 7.2 to make an easy comparison with split TCSC results.

At 90° of firing angle, 1.74% of inductive reactance is possible and -10% of capacitive reactance is at 180°. Less than those values, reactance compensations are not possible in single TCSC. The change in reactance ΔX between 90° to 127° and 180° to 158° in steps of 1° are very small approximately from 0.0082% to 0.4479% respectively; therefore fine tuning of reactance compensation is possible. But in critical region i.e., nearer to resonance, change in reactance starts increasing and gives maximum difference ΔX of 3.1782%; hence fine tuning is not possible. These difficulties can be override by implementing the split TCSC for same degree of compensation k .

Split TCSC is designed so as to get:

(a) Fine tuning of line reactance.

(b) Wide range of compensation.

In split TCSC, k_1 and k_2 are chosen between 1–5% and 9–5% respectively to achieve same 10% degree of compensation k . Both the TCSC's are tuned in steps of 1° of firing angle and '7444' firing points are possible for considered resonance limitation. Fig.7.3 shows split TCSC reactance characteristic curve for $k_1 = 2\%$ and $k_2 = 8\%$ of compensation with respect to number of firing points. The split TCSC reactance can vary from 18.66% to -24.83% for the same resonance region limitation as shown in Fig. 7.1.

Minimum and maximum changes in reactance ΔX are $3.5784 \times 10^{-9}\%$ and 0.3810% respectively. Table 7.1 shows the minimum and maximum change in reactance ΔX at various ratios of k_1 and k_2 .

Fig. 7.4 shows the percentage real power transfer on 19th transmission line with single TCSC installed in IEEE 14 bus system. Real power transfer without TCSC in line no. 19 (i.e., between bus numbers 12 and 13) is 1.6692 MW in base NRPFA. Installing single TCSC on optimally selected 19th line makes the transmission line flexible to transfer real power from 94.41% to 99.46% on inductive side and 103.2% to 108.13% on capacitive side; but tuning of power between 99.46% and 103.2% does not exist.

Considering a split TCSC in place of single TCSC for the same degree of compensation (10%) makes the transmission line more flexible and alters power flow in

wide range. Table 5.2 shows Max. ΔP for IEEE 30 bus system using split TCSC are 0.13% which is very small compared to single TCSC results. It is observed, the split TCSC fine tunes the transmission line reactance for power flow control. The power loss in 19th transmission line is 0.0009 MVA under base NRPFA. With TCSC, losses including portion 94.32–100.9% as shown in Fig. 5.7 which is not possible through single TCSC shown as highlighted portion in Figs. 7.2, 7.4 and 7.6. Thus fine variation in power loss, transfers the power at any fine increment/decrement of dynamic load.

Table 7.1 shows minimum and maximum change in TCSC reactance (ΔX), minimum and maximum change in real power (ΔP), minimum and maximum change in apparent power loss (ΔS_L) for various values of k_1 and k_2 so as to get same 10% of compensation. Amongst all ratios, 2:8 shows best result in fine tuning of line reactance.

Because of same range of compensation $k = 10\%$ and $\omega = 2.4$, same range of power flow is observed in split TCSC as in single TCSC. Merely, split TCSC fine tunes the line power flows. Power flows in all transmission lines are within permissible limits. Fig. 5.8 shows the percentage line loading of each transmission line for single/split TCSC at both extreme compensation levels (18.66% and -24.83%). The transmission line number '10' has maximum power flow of about 67% line load at extreme capacitive compensation of single/split TCSC (-24.83%).

The TCSC device injects inductive/capacitive voltage in series with the transmission line to maintain the voltage stability at light/heavy load condition. The voltage

increased from 100.9% to 108.9% in inductive mode and are decreased from 84.55% to 94.32% in capacitive mode. Fig. 7.6 shows the power loss curve by providing single TCSC. Implementing split TCSC makes the transmission line power loss to vary at fine rate

stability is analyzed for the cases of IEEE 14 bus system without TCSC, with single TCSC and split TCSC. It is verified from Fig. 5.9 voltage profile at buses 12 and 13 are within permissible limits $\pm 5\%$ on both inductive and capacitive mode operations

7.3 ATC Calculation

The Available Transfer Capability (ATC) are computed for a set of source/sink transfers using Continuous Power Flow (CPF). Table 5.3 shows the ATCs for IEEE 14-bus system without TCSC device and with TCSC at both extreme compensation levels (18.66% and -24.83%). The condition of failure is indicated along with the % change in the ATC after TCSC placement at 19th line. It has been observed that there is a decrease of the ATC when TCSC with the extreme compensation level 18.66% compared with the base case and % change is indicated in negative values whereas it has been observed that there is an increase of the ATC when TCSC with extreme compensation level -24.83% compared with based and indicated in positive. It has been observed that increase/decrease of the ATC based on the compensation capacitive/inductive mode.

7.4 Case Study on IEEE 14 bus system

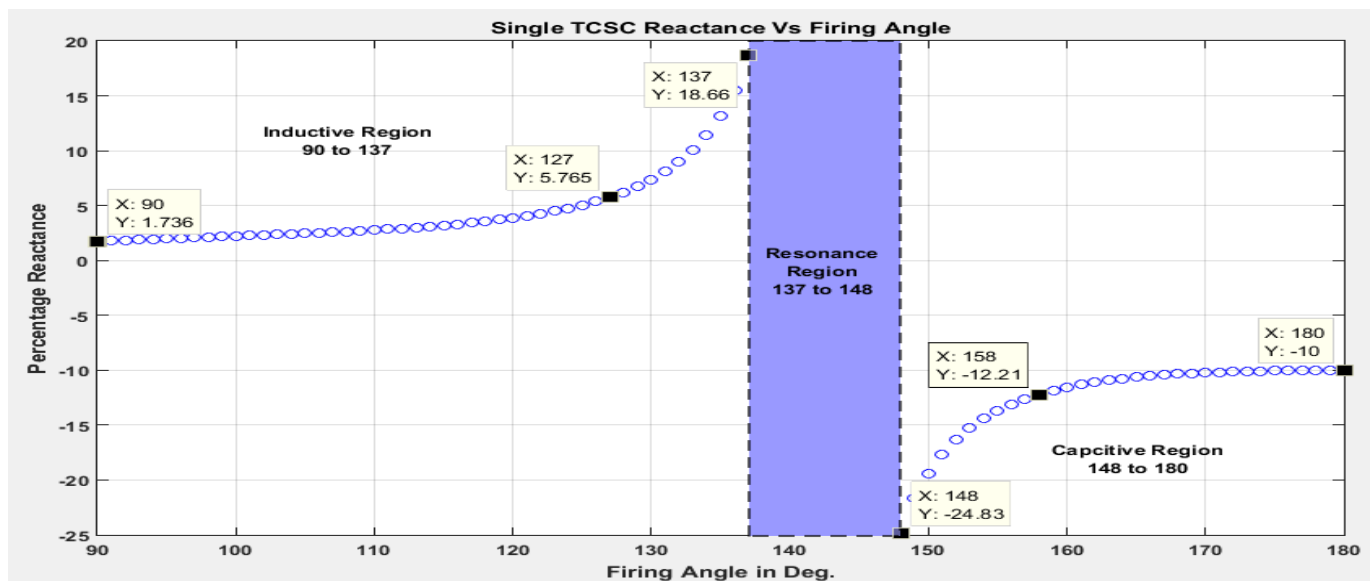


Fig-7.1: Single TCSC reactance characteristic curve in percentage for IEEE 14-bus system

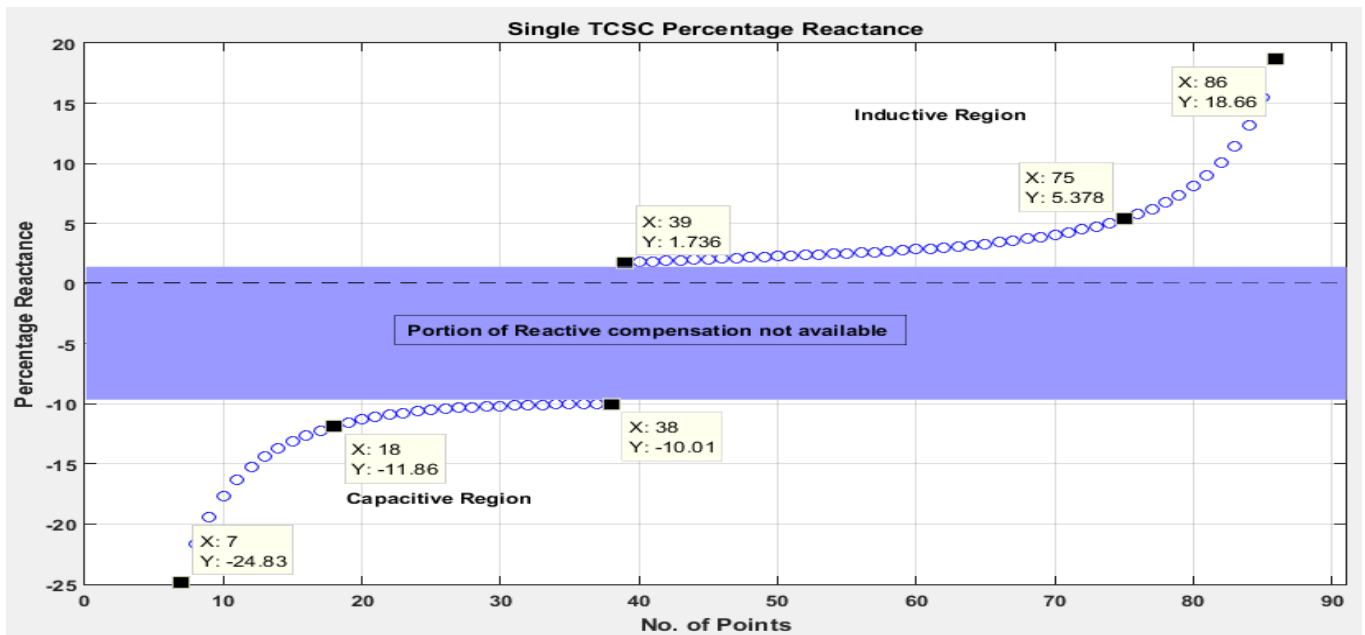


Fig-7.2: Single TCSC reactance characteristic curve plotted with no. of firing steps for IEEE 14-bus system

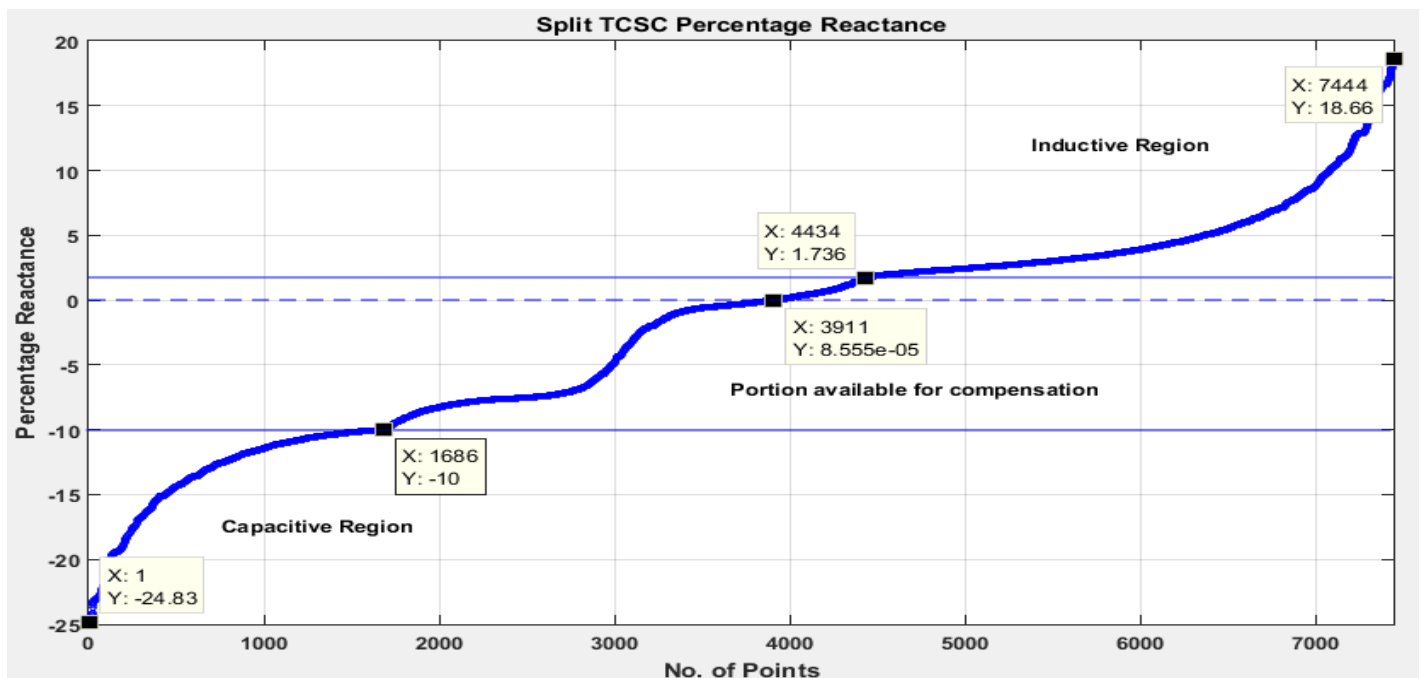


Fig-7.3: Split TCSC reactance characteristic curve in percentage for IEEE 14-bus system

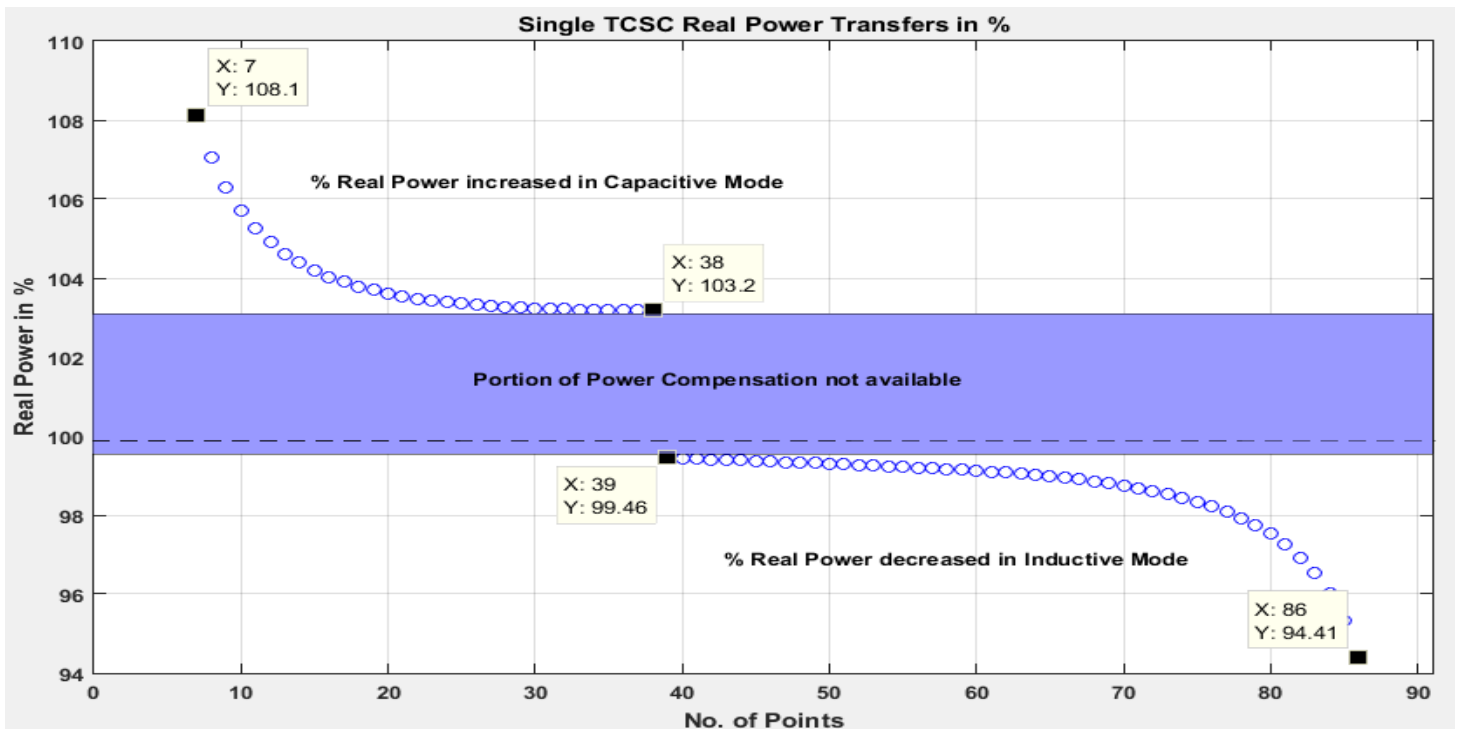


Fig-7.4: Power loss variation in line 19 with single TCSC for IEEE 14-bus system

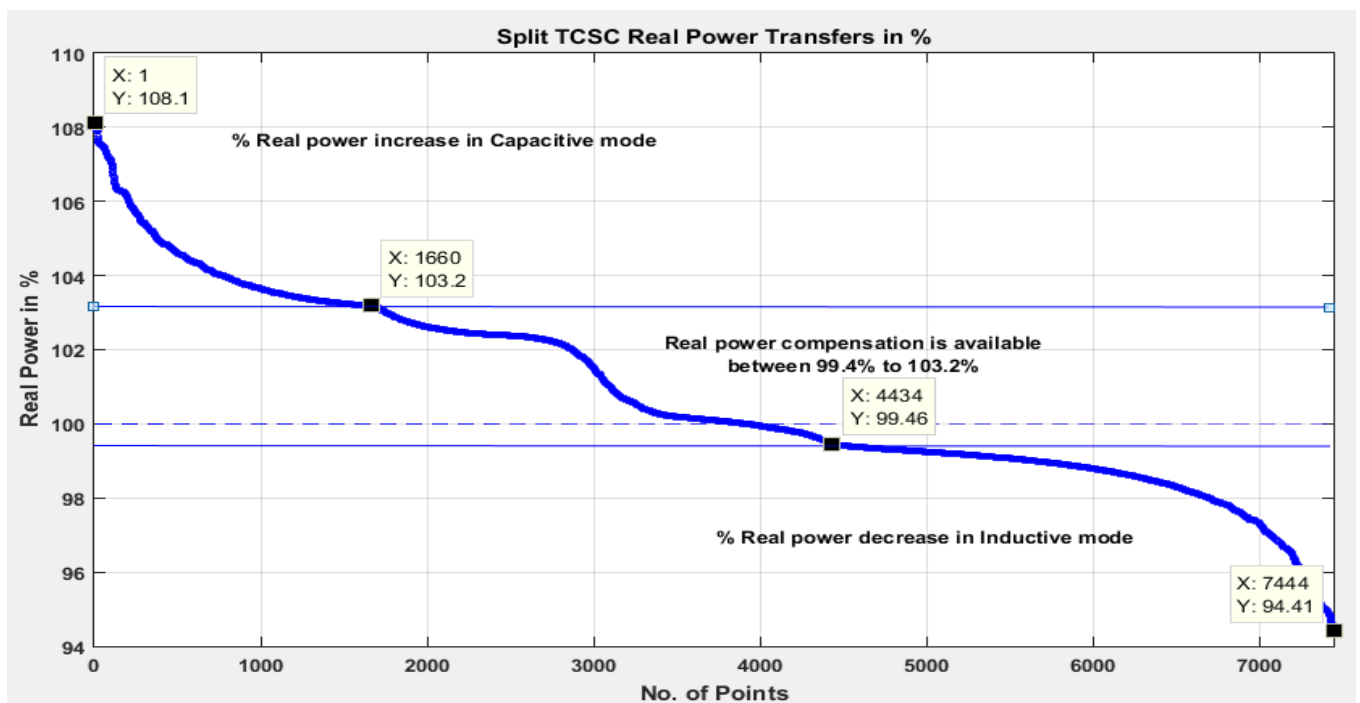


Fig-7.5: Power loss variation in line 19 with split TCSC for IEEE 14-bus system

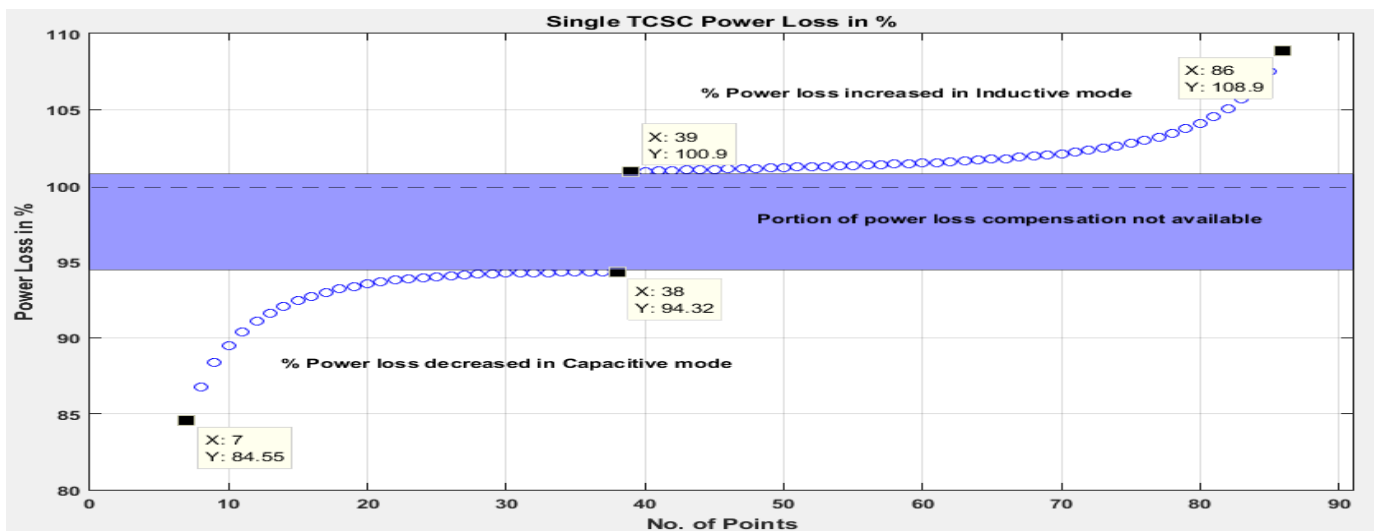


Fig-7.6: Power loss variation in line 19 with single TCSC for IEEE 14-bus system

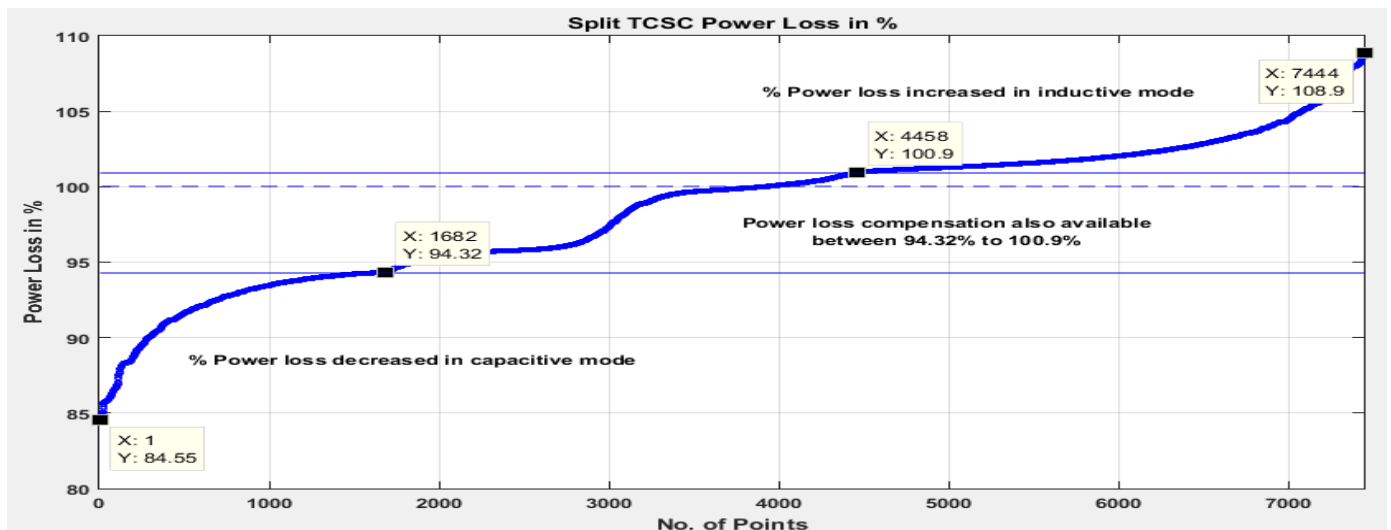


Fig-7.7: Power loss variation in line 19 with split TCSC for IEEE 14-bus system

Table 7.1 Minimum and maximum ΔX , ΔP and ΔS_L for IEEE 14-bus system

Type	Degree of compensation (%)	18.66 < %X < -24.83		94.41 < %P < 108.13		84.55 < %S _L < 108.86	
		% ΔX_{min}	% ΔX_{max}	% ΔP_{min}	% ΔP_{max}	% ΔS_{Lmin}	% ΔS_{Lmax}
Single TCSC	10	0.0090	3.1782	0.0029	1.0804	0.0054	1.5650
Split TCSC	1:9	6.1651e-08	0.3932	1.8956e-08	0.1342	3.1426e-08	0.2766
	2:8	3.5785e-09	0.3810	1.0990e-09	0.1305	2.9234e-09	0.2710
	3:7	2.8428e-07	0.2285	8.5297e-08	0.0706	1.3740e-07	0.1397
	4:6	1.6407e-07	0.3533	5.1615e-08	0.1166	8.6969e-08	0.2423
	5:5	0	0.3083	0	0.0900	0	0.1799

Table 7.2 Test results of IEEE 14 bus system

Parameter	Base NRPF A	With Single TCSC (%)	With Split TCSC (%)
Power Flow	1.6692 MW	94.41 - 99.46 103.18 - 108.13	94.41 - 108.13
Max ΔP	-	1.0804	0.1305

Table 7.3 ATC calculation without and with TCSC extreme compensation levels for IEEE 14-bus system

Seller /Buyer	Base Case		TCSC Inductive Mode (Compensation level 18.66%)			TCSC Capacitive Mode (Compensation level -24.83%)		
	ATC (MW)	Condition failed	ATC (MW)	Condition failed	% Change	ATC (MW)	Condition failed	% Change
6/12	66.2	Line-12 Overflow	64.7	Line-12 Overflow	-2.3	68.4	Line-12 Overflow	3.3
6/13	43.2	Line-13 Overflow	42.7	Line-13 Overflow	-1.2	43.9	Line-13 Overflow	1.6
6/14	69.9	Line-13 Overflow	69.1	Line-13 Overflow	-1.2	71.0	Line-13 Overflow	1.6

8. CONCLUSIONS

This chapter includes the benefits of split TCSC over single TCSC for fine tuning of the line reactance to manage the smooth power flow between lines. This paper explains the incapability of single TCSC at critical region of TCSC characteristic curve and showed the advantage of placing split TCSC over single TCSC for fine tuning of the line reactance. By using split TCSC over single TCSC following advantages are below:

1. Fine tuning of line reactance (which is in micro ohms) based on the loss sensitivity method provides fine control of power flow in the transmission line of IEEE power system.
2. A continuous tuning of line reactance is possible from 18.66% to -24.83% i.e., including portion 1.74% to -10% which is not available in single TCSC. Thus wide range of compensation is offered by split TCSC.
3. By various combinations of tuning the split TCSC in steps of firing angle 1° , 7444 firing points are possible excluding resonance limits 137–148°, as compared to single TCSC where only 83 points are available.
4. ATC of the system is analyzed for the extreme compensation levels and also compared the results with base case by changing the load and generation of 0.001 MW.

Power flow analysis with split TCSC is calculated for various ratios of degree of compensation. Ratio 2:8 showed good results of fine reactance compensation among all.

While simulating NRPF A with single/split TCSC device, all solutions are converged in two iterations with an accuracy of 0.01 for all possible firing angles.

REFERENCES

- [1] McKinsey & Company's Electric Power and Natural Gas Practice, "Powering India: The Road to 2017", executive summary.
- [2] <http://economictimes.indiatimes.com/power/indias-power-demand-to-rise-120-MW-to-135-MW/article-show/3101315.cms>
- [3] Hingorani NG, Gyugyi L. Understanding FACTS concepts and technology of flexible AC transmission systems. IEEE Press, 2000.
- [4] Mathur RM, Varma RK. Thyristor based FACTS controllers for Electrical transmission systems, John Wiley & Sons Inc, 2002.
- [5] Vittal Vijay. Use of series compensation in transmission lines, EE457; 29 April 2004.
- [6] Avramovic B, Fink LH. Energy management systems and control of FACTS. Int J Electric Power Energy Syst 1995;17(3):195-8.
- [7] Kazemi A, Badrzadeh B. Modeling and simulation of SVC and TCSC to study their limits on maximum loadability point. Int J Electric Power Energy Syst 2004:381-8.
- [8] Meikandasivam S, Jain Shailendra Kumar, Nema Rajesh Kumar. Investigation on installed TCSC projects. In: ICEE-2009, PEC, Puducherry, India; 2009.

- [9] Urbanek J, Piwko RJ, Larsen EV, Damsky BL, Furumasu BC, Mittlestadt W, et al. Thyristor controlled series compensation prototype installation at the Slatt 500 kV substation. In: IEEE PES paper 92-SM-467-IPWRD, Seattle; July 1992.
- [10] Narashimha Rao K, Amarnath J, Arun Kumar K. Voltage constrained available transfer capability enhancement with FACTS devices. ARPN J Eng Appl Sci 2007;2(6).
- [11] Taher Seyed Abbas, Besharat Hadi. Transmission congestion management by determining optimal location of FACTS devices in deregulated power systems. Am J Appl Sci 2008;5(3):242-7.
- [12] Arunachalam M, Ghamandi Lal, Rajiv CG. BHEL, Bangalore Babu Narayanan MM, CPRI, Bangalore, India, Performance verification of TCSC control and protection equipment using RTDS. In: 15th PSCC, Liege, 2005, pp. 22-6.
- [13] Meikandasivam S, Nema Rajesh Kumar, Jain Shailendra Kumar. Behavioral study of TCSC device - A MATLAB/simulink implementation. Published in IJEPSE-WASET; Spring 2008, pp. 102-7.
- [14] Hiskens Ian A. Power flow analysis. University of Wisconsin-Madison; November 2006 and 2003.
- [15] Sadat Hadi. Power system analysis. Tata McGraw Hill, 2002, pp. 189-240.
- [16] Wang Feng G, Sherstha B. Allocation of TCSC devices to optimal total transmission capacity in a competitive power market. IEEE Trans 2001:587-93.
- [17] Abdel-Moamen M, Narayana Prasad Padhy A. Power flow control and transmission loss minimization model with TCSC for practical power networks. Power Eng Soc Gen Meet IEEE 2003;2:880-4.
- [18] Mahdad Belkacem, Bouktir Tarek, Srairi Kamel. Strategy of location and control of FACTS devices for enhancing power quality. In: Electrotechnical conference, IEEE, MELECON; 2006. p. 1068-72.
- [19] Biansoongnern S, Chusanapiputt S, Phoomvuthisarn S. Optimal SVC and TCSC placement for minimization of transmission losses. In: International conference on power system technology, 2006, IEEE.
- [20] Ghawghawe a ND, Thakre KL. Computation of TCSC reactance and suggesting criterion of its location for ATC improvement. Int J Electrical Power Energy Syst 2009:86-93.
- [21] Nireekshana T, Kesava Rao G, Siva Naga Raju S. Enhancement of ATC with FACTS devices using real-code Genetic algorithm. Int J Electr Power Energy Syst 2012:1276-84.
- [22] Preedavichit Preecha, Srivastava SC. Optimal reactive power dispatch considering FACTS devices. In: APSCOM-97, Hong Kong; November 1997. pp. 620-5.
- [23] Meikandasivam S, Rajesh Kumar Nema, and Shailendra Kumar Jain. Selection of TCSC parameters: Capacitor and Inductor. In: IICPE-2007, New Delhi, January 2011. pp. 1-5.
- [24] Ajarapu V, Christie C. The continuation power flow: a practical tool for tracing power system steady state stationary behavior due to the load and generation variations. IEEE Trans Power Sys 1992, vol. 7, no. 1 pp.416-23.
- [25] Transmission transfer capability task force, Available transfer capability Definitions and determination, North American Electric Reliability Council, NJ; June 1996.
- [26] Ejebe GC, Tong J, Waight JG, Frame JG, Wang X, Tinney WF. Available transfer capability calculations. IEEE Trans Power Sys 1998, vol. 13, no. 4, pp. 1521-7